Impurity separation efficiency of multi-component wastewater in a pilot-scale freeze crystallizer

John Miia, Choudhury Tuhin, Filimonov Roman, Kurvinen Emil, Saeed Muhammad, Mikkola Aki, Mänttäri Mika, Louhi-Kultanen Marjatta

DOI: 10.1016/j.seppur.2019.116271

Impurity separation efficiency of multi-component wastewater in a pilot-scale freeze crystallizer

Miia John[a,*], Tuhin Choudhury[b], Roman Filimonov[c], Emil Kurvinen[b], Muhammad Saeed[a], Aki Mikkola[b], Mika Mänttäri[a], Marjatta Louhi-Kultanen[d]

[a]*Department of Separation and Purification Technology, LUT School of Engineering Science, LUT University, P.O. Box 20, FI-53850 Lappeenranta, Finland*
[b]*Department of Mechanical Engineering, LUT School of Energy Systems, LUT University, P.O. Box 20, FI-53850 Lappeenranta, Finland*
[c]*Department of Computational and Process Engineering, LUT School of Engineering Science, LUT University, P.O. Box 20, FI-53850 Lappeenranta, Finland*
[d]*Department of Chemical and Metallurgical Engineering, School of Chemical Engineering, Aalto University, P.O. Box 16100, FI-00076 Aalto, Finland*

Abstract

New directions in wastewater treatment consider not only the adequate purification efficiencies but also water and material recovery for recycling and reuse. Freeze crystallization offers the potential for the simultaneous separation of water (ice) and material (i.e., salts and nutrients) from wastewater using a single wastewater purification process. However, the impurity-separation performance of freeze crystallization applied to multi-component wastewaters is still unclear, particularly for industrial or municipal scales.

In this study, a prototype was developed to demonstrate the application of freeze crystallization to wastewater purification on the industrial scale. This freeze crystallizer, a 120 liter jacketed vessel equipped with stirring and ice scraping mechanisms, produced relatively large (500 µm) ice crystals, primarily in water suspension. To evaluate the purification efficiencies of the prototype system, a comprehensive number of water-quality indicators were measured following the purification of highly concentrated landfill leachates. The prototype system achieved a >95% average impurity removal efficiency for both organic and inorganic matter, including heavy metals. This excellent separation ability, given the variety of impurities present in the leachates, shows the non-selective nature of freeze separation for wastewater treatment. These outcomes

*Corresponding author.
E-mail address: miia.john@lut.fi

represent an important step forward in scaling up and developing the full scale freeze purification process for wastewaters.

Keywords: Ice purity; Freeze crystallization; Purification efficiency; Wastewater treatment

1. Introduction

Conventional wastewater treatment systems combine a number of different purification sub-processes to make effluent clean enough to be returned to the environment. Because of urban living and industrial activities, variegated impurities accumulate in waters forming dilute but complex aqueous solutions. Then, the wastewaters are drained and piped long distances to wastewater treatment plants. There, the physical, chemical and biological processes play their unique roles in the purification process with more advanced techniques applied in even more limited operating environments. The complexity of these systems makes it difficult to maintain reasonable energy consumption levels and operating costs. Reducing the overall volume of water being transferred and/or treating the wastewater nearer to its source could help. Moreover, it is becoming increasingly important to address industrial effluents that contain toxics, heavy metals, or other harmful substances, and urban origin wastewaters that contain emerging micropollutants, with more advanced water purification methods.

According to our previous research [1] and the results obtained by Erlbeck et al. [2],Yin et al. [3] and Williams et al. [4], freeze crystallization has many of the attributes needed for efficient and cost effective wastewater treatment. Environmental friendliness is a key benefit, because the freezing process needs no added chemicals, no more waste is generated (as filter media), and toxic waters can be treated. In arctic areas, energy efficiencies can even be higher if the colder temperatures in those environments are properly exploited. In addition to cost savings, the lower operating temperatures associated with freeze crystallization can result in substantially less corrosion. In this study, however, purification efficiencies and the theorized non-selective nature

of impurity separation are of interest. The high separation ability may enable better water and material recovery and recycling in the future. In addition, by freeze crystallization it is possible to reduce the pure water quantity of wastewater concurrently with the wastewater purification process [5].

Existing freeze crystallization methods in wastewater treatment can be divided into three main categories: ice growth in a layer, droplet (spray) freezing, and ice growth in suspension. This study focuses on the latter and in particular on the suspension freeze crystallizer. Bogdan and Molina [6] studied the forming of mixed–phase particles from solution droplets during freezing and observed an ice core forming with a freeze-concentrated solution coating. Similarly, when ice crystallization takes place in an aqueous solution, the formed ice naturally repels impurities leaving a remaining liquid with a concentration of impurities. In a suspension freeze crystallizer, the formed ice particles are dispersed throughout the fluid in the suspension of the mother liquid. The transactions between growing ice crystals and concentrated solution, i.e., how impurities adhere to the ice crystal surface when crystals are forming and floating inside the liquid and how easily impurities are detached during ice separation, determine total impurity removal efficiencies. [7,8].

Previous research concerning suspension freeze crystallizers has often been performed using model or artificial waters instead of real wastewaters and mostly in the laboratory. Moreover, these experiments usually utilize eutectic freeze crystallization (EFC), and they focus more on investigating process parameters and crystal size than on examining purification efficiencies in terms of ice purity [1,9,10]. Experiments conducted on a larger scale are more often carried out using the EFC technique and with industrial effluents or brines as concluded from reviews of freeze crystallization for desalination [3] and reverse osmosis brine treatments [11]. For instance, Rodriguez Pascual et al. [12] and Van Spronsen et al. [13] conducted EFC-tests with scraped and cooled wall crystallizers, volumes of 130 L and 180 L, respectively. Clear purification

efficiencies by ice purity were not presented, as the study was more focused on process control, heat transfer, and carbonate salts production from specific industrial waste solutions.

Suspension freeze crystallization experiments conducted with real wastewater that include purification efficiency studies or extensive impurity analyses are rare. Chang et al. [8] studied freeze desalination by analyzing the major ions from seawater: sodium, magnesium, calcium, and potassium. Their focus was on the salinity limits of potable water so clear impurity removal efficiencies were not determined. Similarly, Erlbeck et al. [2] studied freeze desalination with slightly wider analysis (anions chloride and sulfate in addition) using the Atlantic Ocean seawater and results were presented by concentrations (mg/L) as well. In most studies, the ice formed in wastewater is analyzed using one or two indicators. For instance, Yin et al. [3] and Feng et al. [14] presented a chemical oxygen demand (COD) removal efficiency above 90% with wastewaters from the pharmaceutical industry and waste cutting fluid from a machinery factory, respectively. Similarly, the 98% ice purity from EFC used to treat textile wastewaters was presented in a color and sodium analysis indicating the main impurity, sodium sulfate [15]. Slightly wider analyses with some cation and anion concentrations were conducted via EFC tests with reverse osmosis brine by Randall et al. [10]. However, the purities of the produced sulfate salts and not the clear removal efficiencies were presented. The scarcity of published research where actual wastewaters are treated by freeze crystallization in a reactor might be the result of the complex nature of wastewater matrices, i.e. a multi-component mixture of impurities [16].

The research reported here demonstrates how well the landfill leachate wastewater was purified in the newly developed freeze crystallizer prototype. In a broader context, the objectives were to establish how well the freeze crystallization method separates all types of wastewater impurities (organic and inorganic, soluble and insoluble) and to demonstrate, through extensive analysis, the non-selective nature of the freezing method. The landfill leachate was selected for testing, because it contains a wide variety of impurities.

2. Pilot crystallizer design

Important design basis requirements for the wastewater freeze crystallizer included high separation performance and ease of operation. To ensure mobility, another requirement was to keep the reactor size small enough to accommodate installation in an intermodal container. Proving the freeze crystallization process in the resulting reactor was the basis for all design choices. A process that produces larger ice crystal sizes in lower quantities was targeted to minimize overall ice crystal surface area and, as a result, minimize the percentage of impurities adhering to crystal surfaces [7]. With less contamination, the separation of solid ice from the ice-water slurry is more effective and results in less washing needed. The main driving force in freeze crystallization is temperature difference (ΔT) between the water in the reactor and the coolant [1]. Therefore, the ability to control the water temperature during the crystallization process was considered especially important to process design. Stirring was introduced to keep the water mixed, which improves heat transfer and temperature equalization. Simplistically, stirring directly affects supersaturation, ice nucleation, ice crystal growth, and ultimately ice crystal size [17]. Encrustation, ice scaling on the cooling wall surface, is undesirable for the process; however, the freeze crystallizer prototype was designed with a scraping assembly to prevent the forming of ice scale.

2.1. Freeze crystallizer

Precooling the wastewater input to the freeze crystallization reactor minimizes the cooling load required within the reactor vessel and allows the use of a conventional jacketed vessel even though heat transfer out through the jacketed walls is reduced. Fig. 1 shows the reactor model of the freeze crystallizer used in this study for impurity separation. The water capacity of the vessel is 120 L excluding the non-jacketed conical volume at the base. The jacketed vessel is approximately 1080 mm in height, has an inner diameter of 400 mm, and an outer diameter of 450 mm. Wastewater enters the vessel via an inlet located at the top head of the reactor. The ice

slurry outlet is at the top of the vessel as well. Emptying of the vessel, and sampling of the concentrated water if needed, can be accomplished through the pinch valve with a manual actuator installed at the bottom of the vessel.

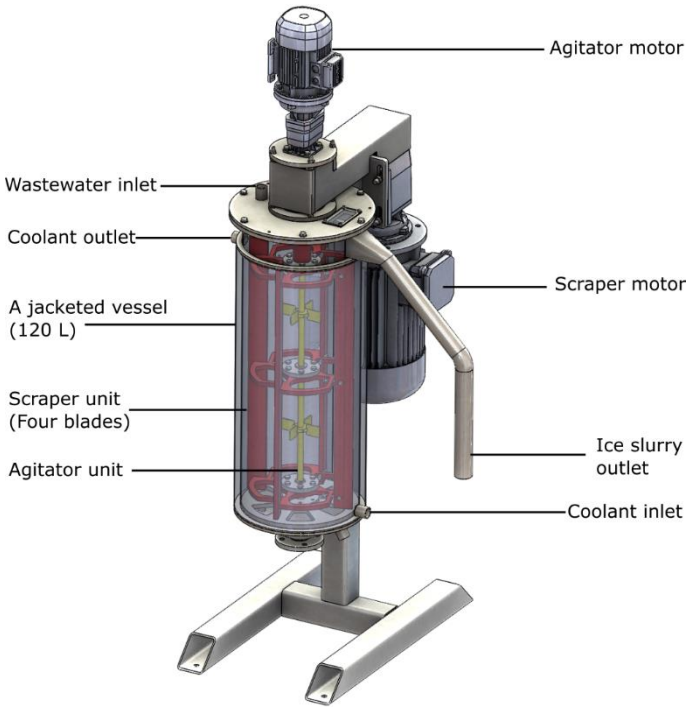

Fig. 1. Pilot-scale reactor and its main components.

The crystallizer operates on the principle of indirect contact freezing. The coolant is pumped into the jacket through the coolant inlet at the bottom (Fig. 1) and is fed out from the top of the jacket. The total amount of coolant, including the pipe and reactor jacket volumes, is 60 L (29 L in the reactor jacket). Because the outer jacket wall is thermally insulated, the flow through of coolant in the jacket induces heat transfer by conduction from the wastewater through the jacket wall to the coolant. The wall comes directly into contact with the coolant; therefore, it induces a local high temperature difference between the inner wall surface of the reactor and the water being cooled. As a result, ice crystals tend to form and adhere to the cold surface of the wall, i.e. ice scaling occurs instead of forming ice crystals in the suspension of the water. Usually, it is difficult to prevent ice scaling or to remove the formed ice layer from the surface of the wall without adding

a scraping mechanism [13]. Furthermore, as the thickness of ice layer increases, it begins behaving like thermal insulation due to the low thermal conductivity of ice, 2.2 W/(m·K) at 0 K [18]. This leads to a reduction of overall heat transfer coefficient between the coolant and water, which works against any further wastewater cooling. The scraping mechanism eliminates the problem by mechanically removing the ice layer before it grows overly thick. Our previous studies [19,20] concerning the ice growing in layers, showed that the purity of the ice layer correlates with the mechanical strength of ice; the purer the formed ice layer, the more force needed to break the ice. Consequently, a scraper operating at high torque is necessary to ensure sufficient scraping force to maintain optimum heat transfer and maximum ice production.

Notwithstanding incorporation of the scraping mechanism, the rate of cooling of the wastewater remains uneven throughout the solution in the reactor. Firstly, the radial distribution of cooling is higher near the surface of the wall than at the center of the vessel. Secondly, the surface close to the inlet point of the coolant is subjected to the maximum amount of cooling. This uneven radial and vertical cooling can be avoided by installing an agitator inside the reactor. By enhancing liquid circulation, the cooling rate of the solution can be improved and a more uniform temperature distribution inside the crystallizer can be achieved [1,21]. The configuration of the agitator impeller was determined using computational fluid dynamics (CFD) modeling (see Supplementary material, CFD simulations). The present reactor employs a dual impeller configuration: two 4-flat-blade disk type radial flow impellers installed equidistantly from the scraper discs (Fig. 2a). The impeller diameter is 150 mm (~0.37 · diameter of the reactor), the blade length is 50 mm, the blade width is 40 mm, and the disk diameter is 55 mm. The agitator was connected to a 1.1 kW motor via a gear-box with a 2.8 gear ratio (BONF C122P-2.8 P90 B3). The axle assembly consists of a nested scraper and agitator axles with mounted bearings at the bottom of the vessel.

The scraper consists of four blades, which are bolted to three equally spaced discs along the length of the reactor (Fig. 2a and 2b). The short hollow shaft at the top of the scraper (Fig. 2a)

connects to a 2.2 kW variable speed motor via a gear-box with a 72.9 gear ratio (Fig. 1). The gear-box provides the required torque (here maximally 800 Nm) while varying the scraper speed between 0 and 20 rpm. With an increase in ice scaling on the walls, torque requirement increases, which is automatically facilitated by the gear-box. Furthermore, based on a study by Nixon et al. [22] on general improvements to an ice scraping edge, a clearance angle of 5° between the cutting edge of the blade and the ice surface results in the least amount of force needed for scraping. This particular feature is incorporated on the scraping edge of the blades, as shown in Fig. 2b, for efficient ice removal.

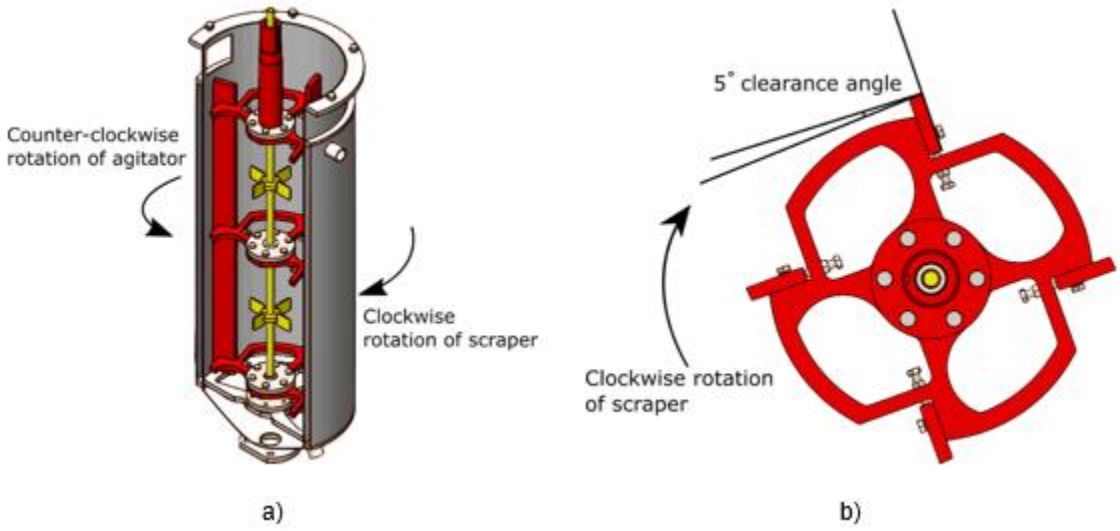

Fig. 2. Section view of the reactor; a) the configuration of the scraper and the agitator, b) the scraper-agitator sub-assembly showing 5° clearance angle for the scraping blade.

The selection of material for the reactor vessel and the auxiliary subassemblies such as the scraper and agitator is another challenging aspect of crystallization reactor design. The reactor requires a material that has high thermal conductivity, such as copper. However, the material must be less reactive to acids or other compounds that might be present in the wastewater. Therefore, AISI 316 grade of stainless steel is considered a suitable alternative. The stainless

steel is also used for the scraper and the agitator as it provides the necessary sturdiness for the structure without compromising on heat transfer.

2.2. Cooling unit

The custom-made cooling device, with a maximum cooling power of 15 kW, comprises a refrigeration unit with a R-134a refrigerant cycle assembled with standard parts. The unit is responsible for circulating monopropylene glycol coolant to the jacket of the reactor with automatic flow control at a minimum flow rate of 10 L/min to a maximum of 60 L/min. The cooling unit is operated and controlled by a Siemens Simatic HMI. The glycol coolant temperature can be preset to any value in the range of -25°C to 25°C with an accuracy of 0.01°C. The nominal coolant temperature is set from 1 to 3°C below the freezing point temperature of the wastewater being treated. An immersion heater was added to the cooling loop for use in emergency cases, such as the scraper jamming in the ice layer or the water in the reactor freezing.

3. Materials and methods

3.1. Wastewater

Freeze crystallization testing was carried out using landfill leachate wastewater taken from the Kukkuroinmäki landfill (Lappeenranta, Finland). The landfill serves as a waste disposal site for non-recyclable waste fractions, and it is situated next to the regional waste management center of Etelä-Karjalan Jätehuolto Oy. Wastewater quality is regularly monitored in compliance with environmental permit regulations. Test wastewater was collected by pumping water from the tank collecting the downward percolation water (due to the precipitation) from the ordinary dry waste bank. Accordingly, the leachate contains constituents dissolved out from the soil fillings and waste materials. The water for the tests was collected in the winter of 2018 when the volume of pumped leachate from the bank is exceptionally low, ~1175 m^3 in a month, as the variation of flow can be 1000-6300 m^3/month. This resulted in an atypically high concentration of impurities in the

leachate. The collected water was transported and stored in 200 L polyethylene plastic barrels and preserved in a cold room at 4°C before use in the experiments.

3.2. Experimental setup

The freeze separation experiments were conducted with the pilot-scale crystallizer and the cooling unit presented above (section 2.) and in Fig. 3. The process parameters for wastewater freezing experiments were chosen based on the preliminary experiments. When the new reactor was initiated, the freezing experiments were conducted using tap water, model sodium chloride solutions and landfill leachate as well. As a result of those tests, it was found that the proper ice generated at the operating temperature of -3°C and high separation efficiency, >95%, was achieved. Since some challenges with the startup of new equipment were faced, as expected, the functional limits for the scraper and agitator were assessed as well. The minimum rotational speeds were found to be 5 rpm and 100 rpm, respectively, since the use of lower speeds induced an overheating of air-cooled motors. In turn, mechanical effects like increased vibration were found to limit the use of higher rotational speeds. Thus, moderate but different scraper rotational speeds of 7 and 10 rpm and agitator rotational speeds of 150, 200 and 250 rpm were chosen for experimental comparison. The frequency converters (1.1 kW and 2.2 kW) were used to control the rotational speed of the agitator and scraper motors (respectively) as well for the control of the direction of rotation. In these experiments, the agitator was rotating anti-clockwise and the scraper clockwise. Table 1 presents the Design of Experiments (DoE) which shows the different scraper and agitator rotational speed combinations used in these tests.

Fig. 3. Freeze crystallizer and cooling unit in the testing environment.

In this study, the freeze crystallization process was operated as a batch process with the residence time of 60 min in every test. The time was counted from the start point of freezing, as the freezing point temperature was reached and ice crystals began to form. The operating temperature (*T)* for the circulating coolant was -3.0°C for every test. This derived the temperature difference (ΔT) between coolant and wastewater to be close to 3°C, as the freezing point depression of the wastewater was measured to be moderate, 0.1°C. The effect of undercooling on freezing was studied by choosing two different ice seeding (i.e., adding of some ice crystals) temperatures, as shown in Table 1. First, the seeding temperature with series C1 was set close

238 to the freezing point temperature -0.06°C (~0°C). With series C2, the wastewater was let to
239 undercool slightly and seeds were added at -0.4°C.

240 **Table 1.** Experimental conditions (DoE) in freeze crystallization tests.

Test	*T* (°C)	*ω*, scraper (rpm)	*ω*, agitator (rpm)
Series C1: Ice seeding at 0 – -0.06°C			
A	-3.0	7	150
B	-3.0	7	200
C	-3.0	7	250
D	-3.0	10	250
E	-3.0	10	150
Series C2: Ice seeding at -0.4°C			
F	-3.0	7	150
G	-3.0	7	200
H	-3.0	7	250
I	-3.0	10	250
J	-3.0	10	150

241

242 The temperature of the water was measured at the bottom of the reactor. A PT 100 sensor
243 (accuracy ±0.015°C, resolution 0.001°C) was connected with a Pico PT-104 Data logger to a PC.
244 The PicoLog software was used for data logging with a 10 s detecting interval as well as online
245 temperature observation on screen during the freezing process. The ice-crystal growth process
246 within the crystallizer was observed visually and by video camera. A bulk endoscope camera
247 YPC110 (resolution 1600x1200, diameter 8 mm, 30 FPS and FOV 70°) was installed on the top
248 of the reactor. An external lamp was used while observing the formed crystals inside the reactor.

3.3. Experimental procedure

A 120 kg batch of well-stirred wastewater was pumped from the barrel container into the crystallizer through the inlet. The wastewater was stored in a cold room, so it had already been precooled to ~4°C. The water was further cooled via refrigeration and coolant circulation through the jacket by setting the coolant temperature to -3°C via the control unit of the cooling device. The process parameters, agitator rotational speed and scraper rotational speed, were set according to the DoE. These settings were kept constant. Ice seeding was performed at a predefined temperature. It was implemented manually by dropping a few ice grains into the water through the inspection hole in the reactor cover. The primary tests showed that the number of ice seeds needed is low, <<0.02% of water volume.

Prior to each freezing test, a sample of the initial wastewater was collected and stored. Immediately after each freeze crystallization test with a residence time of 60 min, the agitator and the scraper were turned off allowing ice to float on the wastewater surface. Several small samples were collected through the top part of the reactor using a small sieve-like sampler (skimmer tool) and combined to make up each sample of formed ice. The collected ice crystals were placed in a 150 mL PP-plastic funnel (with a perforated plate) to drain the excess water. Finally, the samples of “unwashed ice” were combined. For the sample of “washed ice”, the ice crystals were washed three times by filling the funnel with 30 mL cooled tap water (~0°C) to form an ice-water suspension, which was then mixed and drained. Because the intention was to simulate realistic process conditions, no vacuum filtration was used to ensure the slow release and dissolution of the impurities attached to the ice crystals. Some natural melting of the ice also contributed to impurity detachment. The ice and wastewater samples were stored in tightly closed 250 mL PE-plastic bottles in a freeze room at -18°C. Before chemical analysis, the melted ice samples and stored initial wastewater samples were warmed to room temperature.

3.4. Chemical analyses

The initial wastewater and produced unwashed and washed ice samples were analyzed using common water quality measures and methods. A Consort C3040 Multi-parameter analyzer was used to measure pH and electrical conductivity (EC, mS/cm) using a probe with cell constant 1.0 1/cm and range 0.001-100 mS/cm. A HACH DR/2000 spectrophotometer was used to determine chemical oxygen demand (COD, mg/L) via the dichromate oxidation method using 0-150±2.7 mg/L (420 nm) and 0-1500±14 mg/L (620 nm) Spectroquant COD reaction cell test tubes. The same spectrophotometer was used to measure turbidity (FTU) and apparent color (PtCo) via the colorimetric method (450 nm, 455 nm). Total phosphorus (TP, mg/L) of a small number of samples was analyzed using a Merck Spectroquant Nova 60 photometer and photometric test kits for phosphorous.

A wider range of elements was analyzed to investigate the non-selective nature of freeze separation. The concentrations (mg/L) of total organic carbon (TOC), total carbon (TC), inorganic carbon (IC), and total nitrogen (TN) were analyzed with a Shimadzu TOC-L analyzer using the Combustion Catalytic Oxidation/Non-Dispersive Infrared Detection method (detection limit for TC and IC 4 μg/L, for TN 5 μg/L). In total, 25 elements; Au, Ag, Al, As, Bi, Ca, Cd, Co, Cu, Cr, Fe, Hg, K, Mg, Mn, Mo, Na, Ni, Pb, Sb, Se, Te, U, V, and Zn; were analyzed using an Agilent 7700 ICP-MS inductively coupled plasma mass spectrometer. For analysis, the samples were syringed with 0.45 μm pore size cellulose acetate membrane filters. Samples for ICP analyses were diluted with an acid solution (1% HCl, 1% HNO_3). The samples apparently containing a lot of suspended solids were centrifuged at 3000 rpm for 5 minutes before dilution for the ICP analyses.

4. Results and discussion

4.1. Freezing process

Based on acoustic and visual observations made during the experiments, ice growth in the water suspension occurred first followed by ice-scaling layer growth. The scraping sound made as the scraper blades shaved the ice layer from the wall was very clearly perceptible. Based on the initiation of that sound, the freezing time it took to reach 2 mm ice thickness on the cooling wall surface (at some part of the wall) was about 50 minutes with the process parameters used.

The ice mass production goal was 10 kg/h, i.e., 83 kg/(h·m^3). The result after an hour of residence time was 11-12 kg, which was determined by measuring the masses of concentrated water and/or the ice. Accordingly, the mean ice growth rate calculated by measuring total ice mass yield and freezing time was 96 kg/(h·m^3), i.e., 27 g/(s·m^3). This ice mass production rate is similar to results presented in previous studies though with a continuous crystallization process. For instance, Rodriguez Pascual et al. [12] reported 25.6-42 g/(s·m^3) ice production in a cooled wall EFC crystallizer with scraping. The volume of their system, for a sodium carbonate solution, was 130 L. Van der Ham et al. [23] reported 79 kg/(h·m^3) ice production in a cooled disk column crystallizer.

In the present study, since the temperature difference between coolant and water was kept at about -3°C for every test, there was no clear evidence for how the process parameters used affected ice production. It seemed that agitator intensity did influence the onset of ice scaling, but this could not be verified explicitly.

From the temperature measurements, a cooling curve can be drawn and the basic thermodynamics of the freezing process can be clearly presented. Fig. 4 presents the cooling curves (the temperature as a function of time) of the two series C1 and C2, each with different test conditions, measured during the period close the freezing temperatures when water temperatures were <1.5°C. The average cooling rate for all experiments was 0.052°C/min.

Because cooling was linear as a function of the -3°C coolant temperature difference (the main driving force), no significant changes between the slopes can be seen. One minor divergence was seen when a higher 250 rpm stirring speed resulted in lower cooling rates, 0.047–0.049°C/min, in three tests out of four. However, one test gave no clear indication of a stirring effect. Therefore, a clear conclusion regarding this effect could not be made.

Even though temperature differences were small, test results showed that freezing point depression (FPD) temperatures were a function of impurity concentration. By comparing FPDs, the different compositions of the leachate samples in barrels were evident. In the series C1 tests, the average conductivity of the raw feed water was 5.31 mS/cm and the FPD temperature was -0.06°C (Fig. 4a). In the series C2 tests, conductivity was a higher 6.32 mS/cm and FPD temperature was a lower -0.10°C (Fig. 4b). This is likely because of the water sampling procedure in which water was pumped out of the tank in the landfill. The leachate may have been concentrated in layers in the tank.

Between the series C1 and C2 tests, clear undercooling temperature differences were observed as expected. These differences were coincident with the timing of ice seeding. However, no reasonable explanation for how seeding influenced undercooling or the duration of the induction period could be determined. In this study, the induction period was determined as a delay time between ice seeding and the time when freezing point temperature was reached. These times varied between 500 – 1670 s with the series C1 tests and 130 – 500 s with the series C2 tests. The variability is more apparent in series C1, Fig. 4a, where the undercooling (and therefore the induction time too) is strong (~-0.4°C) in two tests and lower in three other tests. The reason might be explained by slow response time of cooling operation and control, or unsuccessful seeding time (with two first series C1 tests). If seed ice is added too soon, it melts and undercooling continues. On the other hand, because wastewater contains many impurities, slight or moderate

undercooling can induce spontaneous ice nucleation. In this case, ice seeding may not be needed at all.

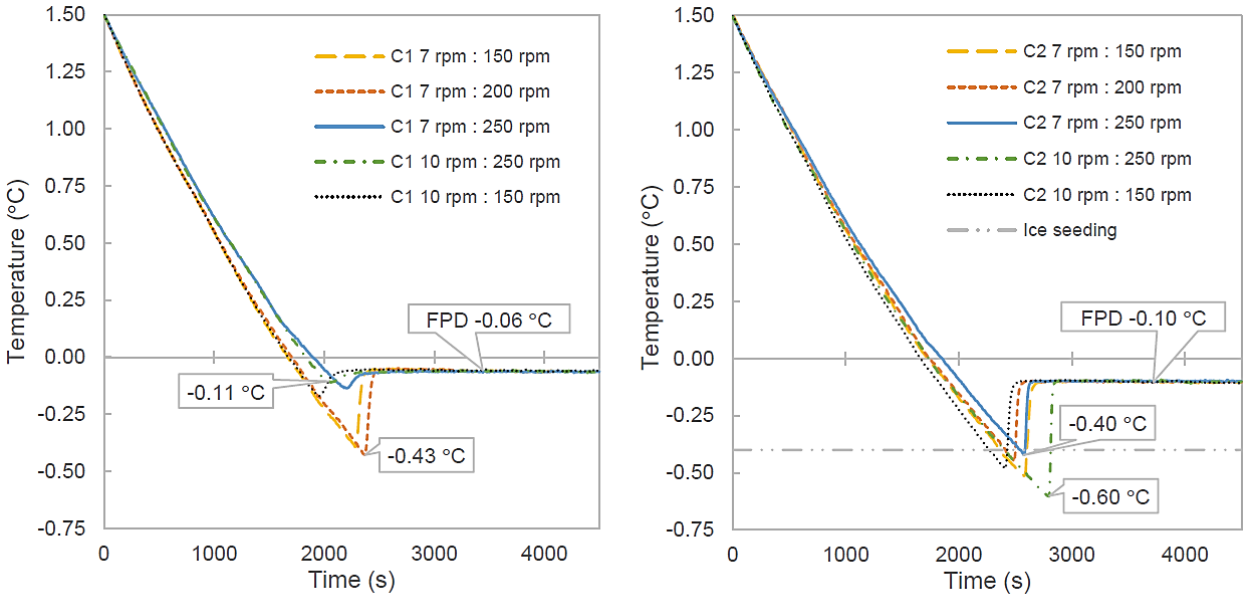

Fig. 4. The cooling curves of freezing processes with different test conditions observed for 75 minutes: (a) Series C1, the ice seeding at ~0 – -0.06°C and (b) Series C2, the ice seeding during the undercooling at -0.4°C.

Median ice crystal size is difficult to measure. In this study, the ice crystal size was visually observed. Microscopic observation (image analysis) using an Olympus BH2-UMA was also used to support the visual observations (Fig. 5a). No clear differences in ice crystal growth (form, size, quantity) resulting from the different processes were apparent. Seeding at close to -0.06°C (practically near to 0°C) and seeding at -0.4°C, formed very irregular and mainly thin plate-shaped ice crystals. The agglomeration of individual ice crystals (forming ice clusters by gathering single crystals together and forming larger crystals) was not detected. Although, this does not exclude the possibility of agglomeration. Shirai et al. [7] discovered that this type of formation had a substantial effect on ice crystal size for longer, one to two hours, residence times. However, Ostwald ripening, when smallest ice crystals melt and larger ice crystals grow further to form bigger crystals, may have possibly taken place - deduced from the crystal size [9,24].

For the most part, the crystals were relatively large, even >500 μm, as shown in Fig. 5, when compared with previous studies. For instance, Van der Ham et al. [23] and Chivavava et al. [9] each produced smaller than 150 μm ice crystals. Washing the ice did not result in a significant crystal size shrinkage effect either (Fig. 5b). To thoroughly evaluate crystal size distribution or ice crystal size evolution during the freezing process, an on-line measurement should have been used. It was also not possible to evaluate the effects on nucleation or ice crystal size of collision, the shear stresses of large crystals, stirring tip speed, or local micro mixing of the scraper [17].

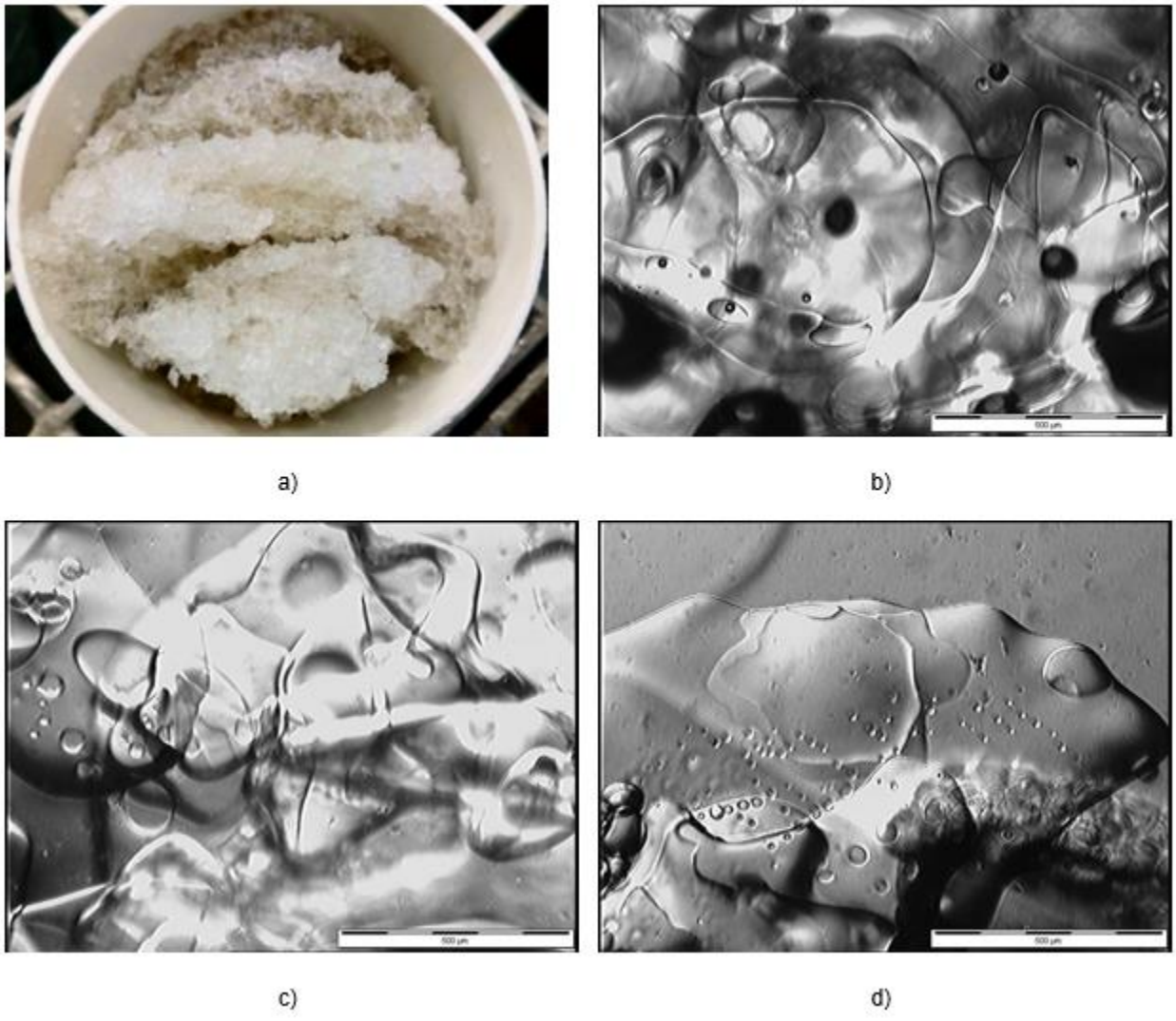

Fig. 5. The characteristics of formed ice crystals; (a) unwashed ice crystals from the series C2 tests formed with an agitator speed of 7 rpm, a scraper speed of 150 rpm, and an ice seeding temperature of -0.4°C; and the microscopic

368 characteristics of; (b) washed ice after 60 min; (c) unwashed ice after 30 min; and (d) unwashed ice after 60 min
369 residence time (bar scale 500 μm in the picture, magnification 5x).

370 **4.2. Separation efficiency**

371 The landfill leachate, used as feed water in this study, proved to contain many compounds in high
372 concentrations at the time of collection. The leachates were similar to high-strength untreated
373 domestic wastewaters, particularly in chemical oxygen demand (COD) and total nitrogen (TN)
374 concentrations [25]. The COD/TOC ratio was 4.6 - 5.3, which indicates that the wastewater
375 contained a lot of organics other than carbon, e.g., nitrogen, phosphorus, or sulphur as well.
376 However, the total phosphorus concentration was low (1.1 – 1.6 mg/L).

377 On the contrary, the high electrical conductivities measured, 5.3 - 6.3 mS/cm, indicate high ionic
378 inorganics content. The density of the landfill leachate was close to that of water. The calculated
379 average results of the analyzed water quality indicators for both test series (and containers) are
380 presented in Table 2. Even though the leachate was collected at the same time, the water content
381 differed in the different storage containers used in the test series. The tested water was slightly
382 alkaline, being very suitable for device structure materials. The detailed, relevant results of
383 measurements and analyses in this study for wastewater, washed ice, and unwashed ice samples
384 are shown in the supplementary material (Supplementary material, Table A.1, A.2, A.3 and A.4).
385 Several analyzed elements are not presented in the results due to the very low concentrations
386 under the detection limits of the method used.

387 **Table 2.** Analyzed results of the initial wastewater (landfill leachate) content averagely in test series.

Test	pH	COD (mg/L)	Conductivity (mS/cm)	Color (PtCo)	Turbidity (FTU)	TOC (mg C/L)	TN (mg N/L)	TP (mg P/L)
Series C1	8.31	811	5.313	1140	278	154	169	1.60
Series C2	7.97	829	6.323	1616	313	180	224	1.10

388

The separation (purification) efficiency of the freeze crystallization can be evaluated by determining the impurity reduction due to the process. Conversely, the effective distribution coefficient *K* indicates the relative part of the impurity quantity remaining in the ice and is calculated by $K = C_i/C_w$, where C_i is the concentration (mg/L) or other measuring value of the substance or the element in melted ice, and C_w is the concentration of the substance or the element in the initial wastewater. Fig. 6 shows the calculated average effective distribution coefficient *K* results for water quality measures COD, EC, color, and turbidity as well as carbon TOC, TC, IC, and nitrogen TN content, for both washed ice and unwashed ice samples. The purification was found to be more efficient with the series C2 tests (Fig. 6b), which were conducted with a higher degree of undercooling. The washed ice of series C1 showed an average efficiency for all these quality measures of 0.110 (89.0%), whereas the series C2 showed 0.027 (97.3%). The variation in the efficiency results between the different tests was also more extensive with the series C1 tests (A to E) than with the series C2 tests (F to J). The freeze separation process was better balanced when a slight undercooling affected the nucleation.

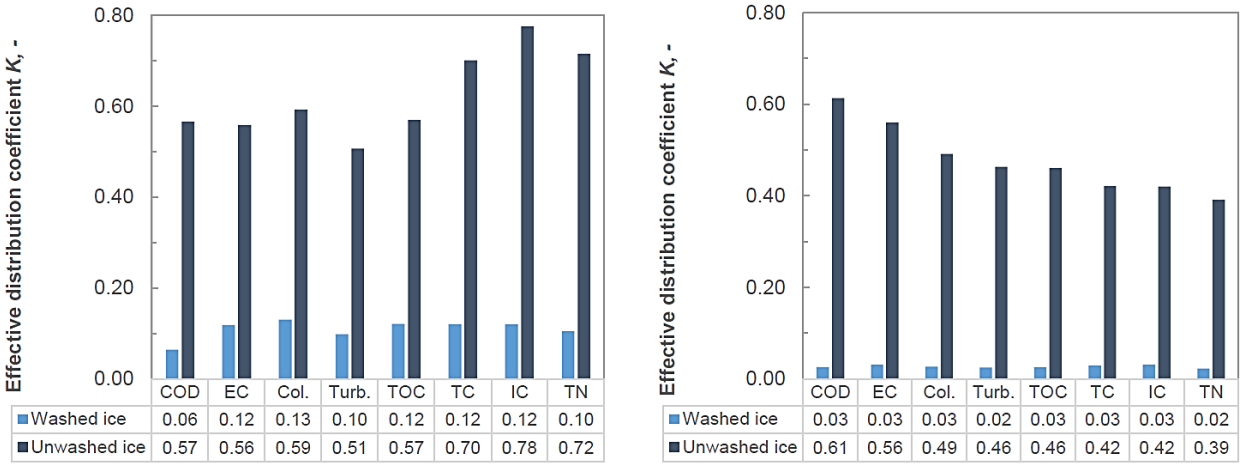

Fig. 6. Average results of test series a) C1 and b) C2 – Determined effective distribution efficiency *K* of chemical oxygen demand COD, electric conductivity EC, color (Col.), turbidity (Turb.), total organic carbon TOC, total carbon TC, inorganic carbon IC, and total nitrogen TN.

Ice washing was found to be of critical importance in ice sample handling - as expected based on the previous research by Lemmer et al. [5], Randall et al. [10,15], and Chang et al. [8]. Even though this study did no focus on the washing procedure as such, Fig. 6a and 6b clearly show the difference between washed and unwashed ice in effective distribution coefficient results. Without washing, the degree of $K = 0.50$ (50%) in efficiency is hardly achievable. Binding conclusions about the ice purity produced cannot be made based only on analyzing the results of the unwashed ice samples. Even though the impurities seemed to be very unequally distributed on the ice crystal surfaces, the effective separation distribution K will be leveled out by washing. Unfortunately, using tap water in ice washing resulted in copper Cu and zinc Zn contamination. The unexpectedly poor water quality from the used tap was only revealed after analysis (Supplementary material, Table A5) and the affected results were excluded. Furthermore, silver Ag, bismuth Bi, and lead Pb contamination occurred as well. However, these elements were present in such low concentrations that they are not covered in the results. The influence of ice polishing (e.g., washing) on the complete purification efficiency evaluation with wastewater would be worth detailed experimental research in the future. In terms of economy, alternative post-treatment methods other than ice washing should be considered as well. For instance, Erlbeck et al. [26] reported recently favorable results in the separation performance of salt solutions treated by a newly designed crystallizer. The process plant incorporates a screw conveyor for ice pressing which brings about the efficient separation of pure ice from an ice/brine mixture.

The separation and purification results for the various elements in the leachates are in line with the water quality results presented above. Because the elemental concentrations of the wastewaters studied vary greatly, from ppb to ppm, the effective separation distribution K results are presented in two different figures (Fig. 7a and 7b) sorted by a concentration scale and shown here only with washed ice samples. The average K values of all elements were 0.168 (83%) for series C1 and a much better 0.050 (95%) for series C2. However, there was no significant

difference in the average *K* values for the elements between the high and low concentrations - the efficiencies were equivalent. The *K* values of calcium Ca and nickel Ni were quite different (almost double) from the average *K* values. This is probably the result of contamination during analysis or from the steel structures and not a function of freezing process characteristics. Of the analyzed elements, the sodium Na (>600 mg/L) and potassium K (<210 mg/L) concentrations were found to be highest in the initial wastewaters. Regardless, the average purification efficiencies were high in series C2: 97.8% and 97.7%, respectively. In conclusion, the freeze crystallizer separated all analyzed impurities of landfill leachate with fairly equal efficiency in similar process conditions.

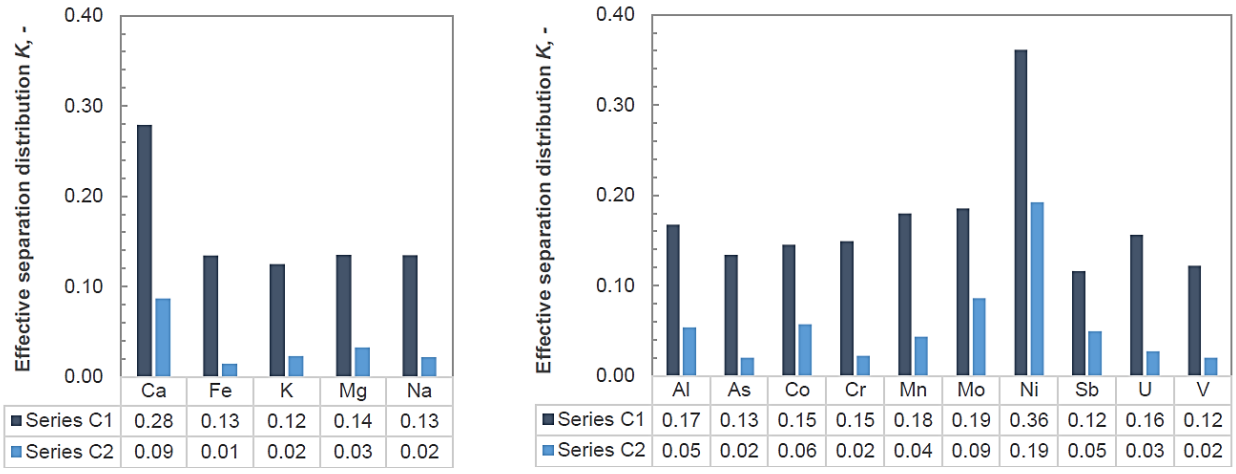

Fig. 7. Average results of test series showing the effective distribution efficiency *K* of various elements with a) higher concentrations (>1.5 mg/ L to 690 mg/L) and b) lower concentrations (<0.5 mg/L) in initial wastewater.

Even though the timing of ice seeding by slightly undercooling was found to have an effect on separation efficiency, the other process parameters did not have an obvious effect. The agitator rotational speed (150, 200, or 250 rpm), scraper rotational speed (7 or 10 rpm) or a combination of these did not influence separation efficiency. The effect of the operating (i.e., freezing) temperature was not studied here, because the temperature used here was selected based on previous tests with model solutions to ensure controlled ice formation. Freezing in different

450 temperatures and varying the other parameters across a broader should also be investigated to
451 find limits and limitations for the freeze crystallizer. The optimization of operation temperature and
452 its influence on purification efficiency should also be more closely examined. The -3°C operation
453 temperature is relatively low. It represents the maximal nominal coolant temperature. Better total
454 energy efficiency is likely achievable at higher freezing temperatures, however, ice production
455 would decrease.

456 It is difficult to compare the purification efficiencies seen in the study with those achieved in
457 previous large-scale freeze crystallization research studies, because of the significant variations
458 in experiment setups, used water quality (seawater, industrial and model water etc.), reactor size,
459 and the undefined tip speeds of stirring. Moreover, previous studies concern mostly eutectic
460 freeze crystallization, and the analyses of impurities focused on salt recovery [12,13]. Previous
461 laboratory-scale studies have mostly resulted in similar purification efficiencies (>95 %). For
462 instance, Yin et al. [3] reported a 70 - 90% COD removal efficiency with highly concentrated
463 pharmaceutical industrial wastewater in a 500 mL suspension crystallizer with an optimal 300 rpm
464 stirring speed at -6°C. Eutectic freeze crystallization using a cascading concentrating process for
465 textile wastewater treatment was investigated by Randall et al. [15] with a 1.5 L jacketed
466 crystallizer, a 350 rpm stirring speed, and a 5°C temperature difference (ΔT). The 98% ice purity
467 was determined based on sodium concentration and color.

468 The legislation and norms for wastewater treatment and the requirements for sufficient purification
469 efficiencies are complicated and vary globally. In Finland, for instance, the environmental impact
470 of a wastewater treatment plant is assessed site-specifically based on the Environmental
471 Protection Act and the Water Act. This means that every plant has a specific environmental permit
472 defining the limits for emissions. These limits are more often significantly stricter than is regulated
473 by the direct law (Government decree on Urban Waste Water Treatment 888/2006, Ministry of
474 Environment, Finland), and they will become even more stringent in the future. For that reason, it

is difficult to determine if the purification efficiencies achieved via freeze crystallization in this study will be sufficient to satisfy future purification requirements. However, purification efficiencies of over 95% for wastewaters with a great variety of impurities have now been achieved using a novel apparatus. Further development of the equipment and the processes should provide even higher purity levels.

5. Conclusions

This study introduced a wastewater purification process based on the freeze crystallization. The prototype crystallizer employs a 120 L jacketed vessel equipped with an agitator and an ice scraper. The design of the freeze crystallizer and the up scaling of a freeze separation process proved successful. An average ice mass production of 96 kg/(h·m^3) was achieved using fixed process conditions and the residence time of 60 min. Most of the ice formed in suspension in the water since ice scale began to form on the cooling wall surface only after 50 min freezing time. The formed ice crystals were relatively large, ~500 μm, which can be seen as an indicator of ice crystal ripening during the process.

The wastewater treatment device purified highly concentrated landfill leachate with appropriate efficiency. With ice washing, average purification efficiencies were >95 - 97%. Without washing, efficiencies of barely 50% were attained. The purification efficiency analyses considered organics (COD, TOC, TN), inorganics (IC, conductivity), and elements such as heavy metals. For the future research, the development and testing of the continuous freeze crystallization process to improve energy efficiency with suitable sub-processes, such as precooling, cold heat recovery, and recycling, as well as the study and development of ice crystal polishing techniques could be considered. Also, testing the crystallizer as an EFC process with salt and nutrient recovery would be of interest.

Declaration of Competing Interest

The authors declare that they have no known competing financial interests or personal relationships that could have appeared to influence the work reported in this paper.

Acknowledgements

The research was funded by the Business Finland, project no. 4591/31/2016. The authors wish to thank Heidi Oksman-Takalo and Sami Huotari, Etelä-Karjalan Jätehuolto Oy, and Hannu Pesonen, Lakeuden Kylmätekniikka Oy, for their collaboration. The authors wish to acknowledge CSC-IT Center for Science, Finland, for providing computational resources. The contributions of Tuomas Nevalainen, Mikko Huhtanen, Toni Kangasmäki and Scott Semken as well as the earlier contribution of Mehdi Hasan during the project are greatly acknowledged.

Appendix A. Supplementary material

Supplementary material related to this research can be found at https://...

References

[1] M. Hasan, R. Filimonov, J. Chivavava, J. Sorvari, M. Louhi-Kultanen, A. Lewis, Ice growth on the cooling surface in a jacketed and stirred eutectic freeze crystallizer of aqueous Na2SO4 solutions, Sep. Purif. Technol. 175 (2017) 512-526. https://doi.org/10.1016/j.seppur.2016.10.014.

[2] L. Erlbeck, M. Rädle, R. Nessel, F. Illner, W. Müller, K. Rudolph, T. Kunz, F.-J. Methner, Investigation of the depletion of ions through freeze desalination, Desalination 407 (2017) 93–102. https://doi.org/10.1016/j.desal.2016.12.009.

[3] Y. Yin, Y. Yang, M. de Lourdes Mendoza, S. Zhai, W.L. Feng, Y. Wang, M. Gu, L. Cai, L. Zhang, Progressive freezing and suspension crystallization methods for tetrahydrofuran recovery

519 from Grignard reagent wastewater, J. Clean. Prod. 144 (2017) 180-186.
520 https://doi.org/10.1016/j.jclepro.2017.01.012.

521 [4] P.M. Williams, M. Ahmad, B.S. Connolly, D.L. Oatley-Radcliffe, Technology for freeze
522 concentration in the desalination industry, Desalination 356 (2015) 314-327.
523 https://doi.org/10.1016/j.desal.2014.10.023.

524 [5] S. Lemmer, R. Klomp, R. Ruemekorf, R. Scholz, Preconcentration of wastewater through the
525 Niro freeze concentration process, Chem. Eng. Technol. 24(5) (2001) 485-488.
526 https://doi.org/10.1002/1521-4125(200105)24:5<485::AID-CEAT485>3.0.CO;2-H.

527 [6] A. Bogdan, J. Molina, Physical chemistry of the freezing process of atmospheric aqueous
528 drops, J. Phys. Chem. A 121(16) (2017) 3109-3116. https://doi.org/10.1021/acs.jpca.7b02571.

529 [7] Y. Shirai, T. Sugimoto, M. Hashimoto, K. Nakanishi, R. Matsuno, Mechanism of ice growth in
530 a batch crystallizer with an external cooler for freeze concentration, Agr. Biol. Chem. 51(9) (1987)
531 2359-2366. https://doi.org/10.1080/00021369.1987.10868410.

532 [8] J. Chang, J. Zuo, K-J. Lu, T-S. Chung, Freeze desalination of seawater using LNG cold energy,
533 Water Res. 102 (2016) 282-293. https://doi.org/10.1016/j.watres.2016.06.046.

534 [9] J. Chivavava, M. Rodriguez Pascual., A.E. Lewis, Effect of operating conditions on ice
535 characteristics in continuous eutectic freeze crystallization, Chem. Eng. Technol. 37(8) (2014)
536 1314-1320. https://doi.org/10.1002/ceat.201400094.

537 [10] D.G. Randall, J. Nathoo, A.E. Lewis, A case study for treating a reverse osmosis brine using
538 Eutectic Freeze Crystallization – approaching a zero waste process, Desalination 266 (1-3) (2011)
539 256-262. https://doi.org/10.1016/j.desal.2010.08.034.

[11] D.G. Randall, J. Nathoo, A succinct review of the treatment of Reverse Osmosis brines using Freeze Crystallization, J. Water Proc. Eng. 8 (2015) 186-194. https://doi.org/10.1016/j.jwpe.2015.10.005.

[12] M. Rodriguez Pascual, F.E. Genceli, D.O. Trambitas, H. Evers, J. Van Spronsen, G.J. Witkamp, A novel scraped cooled wall crystallizer: Recovery of sodium carbonate and ice from an industrial aqueous solution by eutectic freeze crystallization, Chem. Eng. Res. Des. 88(9) (2010) 1252-1258. https://doi.org/10.1016/j.cherd.2009.07.015.

[13] J. Van Spronsen, M. Rodriguez Pascual, F.E. Genceli, D.O. Trambitas, H. Evers, G.J. Witkamp, Eutectic freeze crystallization from the ternary Na2CO3–NaHCO3–H2O system: A novel scraped wall crystallizer for the recovery of soda from an industrial aqueous stream, Chem. Eng. Res. Des. 88(9) (2010) 1259-1263. https://doi.org/10.1016/j.cherd.2009.09.012.

[14] W. Feng, Y. Yin, M. De Lourdes Mendoza, L. Wang, P. Chen, Y. Liu, L. Cai, L. Zhang, Oil recovery from waste cutting fluid via the combination of suspension crystallization and freeze-thaw processes, J. Clean. Prod. 172 (2018) 481-487. https://doi.org/10.1016/j.jclepro.2017.09.281.

[15] D.G. Randall, C. Zinn, A. E. Lewis, Treatment of textile wastewaters using Eutectic Freeze Crystallization, Water Sci. Technol. 70(4) (2014) 736-741. https://doi.org/10.2166/wst.2014.289.

[16] O. Lorain, P. Thiebaud, , E. Badorc, Y. Aurelle, Potential of freezing in wastewater treatment: Soluble pollutant applications. Water Res. 35(2) (2001) 541-547. https://doi.org/10.1016/S0043-1354(00)00287-6.

[17] A. Mersmann, Crystallization technology handbook, second ed., New York: Dekker, 2001.

[18] J.R. Rumble (Ed.), CRC Handbook of Chemistry and Physics, 99th ed., CRC Press/Taylor & Francis, Boca Raton, FL, Internet Version 2018.

563 [19] M. John, M. Suominen, O-V. Sormunen, M. Hasan, E. Kurvinen, P. Kujala, A. Mikkola, M.
564 Louhi-Kultanen, Purity and mechanical strength of naturally frozen ice in wastewater basins,
565 Water Res. 145 (2018) 418-428. https://doi.org/10.1016/j.watres.2018.08.063.

566 [20] M. John, M. Suominen, E. Kurvinen, O-V. Sormunen, M., Hasan, P. Kujala, A. Mikkola, M.
567 Louhi-Kultanen, Separation efficiency and ice strength properties in simulated natural freezing of
568 aqueous solutions, Cold Reg. Sci. Technol. 158 (2019) 18-29.
569 https://doi.org/10.1016/j.coldregions.2018.11.006.

570 [21] S. Palosaari, M. Louhi-Kultanen, Z. Sha, Industrial Crystallization, in: A.S. Mujumdar (Ed.),
571 Handbook of industrial drying, fourth ed., CRC Press Inc., (2014) pp. 1271-1290.

572 [22] W.A. Nixon, T.J. Gawronski, A.E. Whelan, Development of a model for the ice scraping
573 process, IIHR Technical Report No. 383, Iowa Institute of Hydraulic Research, 1996.

574 [23] F. Van der Ham, M.M. Seckler, G.J. Witkamp, Eutectic freeze crystallization in a new
575 apparatus: the cooled disk column crystallizer, Chem. Eng. Process.: Process Intensification
576 43(2) (2004) 161-167. https://doi.org/10.1016/S0255-2701(03)00018-7.

577 [24] A.S. Myerson, Handbook of industrial crystallization, second ed., Boston (MA): Butterworth
578 Heinemann, 2002.

579 [25] G. Tchobanoglous, F.L. Burton, D.H. Stensel, Wastewater engineering: Treatment and reuse,
580 fourth ed., McGraw-Hill, New York, 2003.

581 [26] L. Erlbeck, D. Wössner, K. Schlachter, T. Kunz, F.-J. Methner, M. Rädle, Investigation of a
582 novel scraped surface crystallizer with included ice-pressing section as new purification
583 technology, Sep. Purif. Technol. 228 (2019) 115748.
584 https://doi.org/10.1016/j.seppur.2019.115748.